
Since January 2020 Elsevier has created a COVID-19 resource centre with free information in English and Mandarin on the novel coronavirus COVID-19. The COVID-19 resource centre is hosted on Elsevier Connect, the company's public news and information website.

Journal of Infection xxx (xxxx) xxx

Contents lists available at ScienceDirect

Journal of Infection

journal homepage: www.elsevier.com/locate/jinf

Letter to the Editor

## RBD-ACE2 binding properties in five SARS-CoV-2 variants of concern with new perspectives in the design of pan-coronavirus peptide inhibitors

*Dear Editor*,

In this journal, Fantini et al. highlighted the important role of structural dynamics in COVID-19 monitor.[1] It is well known that the recent increase in COVID-19 cases is directly related to novel variants of SARS-CoV-2. The WHO announced a total of five SARS-CoV-2 variants of concern (VOCs), i.e. alpha, beta, gamma, delta and omicron variants, until September 8, 2022. The mutation information on the receptor-binding domains (RBDs) of the aforementioned variants is shown in Supplementary Fig. 1. VOCs are often accompanied by enhanced transmissibility and virulence, and may result in the reduced effectiveness of current diagnostic methods, treatment regimens or vaccines, and are therefore focal points of research.[2] In response to the issues concerning researchers, the binding properties of RBDs in five SARS-CoV-2 VOCs to angiotensin-converting enzyme 2 (ACE2) were studied by two independent molecular dynamics (MD) simulations and various analytical methods to design a pan-coronavirus peptide inhibitor against the variant-strains.[3–5] This study is expected to provide useful references and new perspectives on the prevention and treatment of COVID-19.

Based on the equilibrium trajectory (50-100 ns) in Supplementary Fig. 2, cross-correlation matrices and porcupine plots of RBDs in all systems were constructed to observe the mutation-induced changes in the internal dynamics of proteins, as shown in Fig. 1. Mutations resulted in an enhancement of positive or negative correlated motions between residues, and several locations were particularly evident, which are marked by red circles, including: (1) Correlated movements of residues near Y453-L455 relative to residues near K417-I418 and D420-Y423 in the alpha RBD (Fig. 1B). It was found that the motion strength of residues near Y453-L455 was significantly enhanced, and the motion directions of residues near K417-I418 and D420-Y423 were more consistent with those of residues near Y453-L455 (Fig. 1G). Meanwhile, the motion directions of residues near N460-E465 and A419-I425 tended to be more consistent than those in the original RBD, thus leading to an enhancement of correlated motion between them. A similar phenomenon also occurred in the beta and gamma RBDs. (2) Anti-correlated movements of residues near C480-G482 relative to residues near N422, Y453-L455, E465 and Y489-L492 in the alpha RBD, which are attributed to the change in the movement pattern of residues near C480-G482. (3) Anti-correlated movements of residues near G482-E484 relative to residues near Y421 and F456-R457 in the beta RBD (Fig. 1C), and residues near D389-C391 relative to residues near C379-G381 and T430-V433 in the gamma RBD (Fig. 1D). (4) The anti-correlated movement of residue Y369 relative to residue Q506 in the delta RBD (Fig. 1E). (5) Anti-correlated movements of residues near C361-A363 relative to residues near F347-S349, I434, S438-D442, Y508-V512 and D398-S399 in the omicron RBD (Fig. 1F). Changes in motion direction of residues contributed greatly to the increase in the anti-correlated motion of residues (Fig. 1K). (6) Anti-correlated movements of residues near N394-V395 relative to residues near S366 and Y369, and residue R403 relative to residue Y365 in the omicron RBD. The main reason for phenomena (3), (4) and (6) is the enhanced movement strength of residues (Fig. 1H, 1I, 1J and 1L).

Subsequently, the binding free energy between the RBDs and ACE2 was calculated by MM-PBSA method (Fig. 2A). From this analysis, it can be concluded that the five SARS-CoV-2 VOCs have enhanced binding ability to host receptor, and the delta and omicron variants have the strongest interactions with the host. This simulation result is highly consistent with the experimental results.[6] Then, each term of the binding free energy was analyzed to determine the main driving force for the above-mentioned binding differences, including van der Waals interaction ($\Delta E_{vdw}$), electrostatic interaction ($\Delta E_{ele}$), polar solvation free energy ($\Delta G_{pb}$) and non-polar solvation free energy ($\Delta G_{np}$). As shown in Fig. 2A, the enhancement of the binding affinity of the alpha, beta and gamma RBDs to ACE2 was dominated by van der Waals interactions, while that of delta and omicron RBDs to ACE2 was controlled by van der Waals and polar interactions. The energy contribution of each residue on the RBD and ACE2 was subsequently calculated, and the results showed that: (1) mutations N501Y, E484K, E484A, T478K, Q493R, Q498R, N440K and S477N promoted ACE2-binding ability of the corresponding variants, mutations K417N/K417T, G496S and Y505H adversely affected it, and mutations L452R, G339D, S371L, S373P and S375F had little influence (Fig. 2B and Supplementary Fig. 3); (2) residues at positions 493, 501, 505, 486, 487, 502, 408, 475, 455, 500 and 456 of the RBD, and residues K353, K31, H34, T27, Y41, Q24, Y83, F28, R393, L79, M82, R357 and G354 of ACE2 were important for the tight binding of all investigated SARS-CoV-2 strains to ACE2 (Fig. 2B and Supplementary Figs. 3–4 and 7); (3) compared with the original SARS-CoV-2 RBD, the preferential binding of the alpha, beta, gamma, delta and omicron RBDs to ACE2 was determined by ten (E484, F486, Y489, F490, L492, Q493 and $Y501^{N}$ in alpha RBD, and T27, K31and L79 in ACE2), fifteen (Y449, Y473, A475, G476, $K484^{E}$, F486, Y489 and $Y501^{N}$ in beta RBD, and S19, Q24, K26, D30, H34, E35 and E37 in ACE2), four ($K484^{E}$ and $Y501^{N}$ in gamma RBD, and D30 and E35 in ACE2), sixteen (Y449, G476, $K478^{T}$, F486, Y489, Y495 and N501 in delta RBD, and Q24, T27, D30, H34, E35, E37, Y41, K353 and D355 in ACE2) and sixteen ($K440^{N}$, Y449, $N477^{S}$, $K478^{T}$, $A484^{E}$, F490, $R493^{Q}$, $R498^{Q}$ and

*Abbreviations:* VOCs, Variants of concern; ACE2, Angiotensin-converting enzyme 2; MD, Molecular dynamics; RBDs, Receptor-binding domains.

https://doi.org/10.1016/j.jinf.2022.09.011

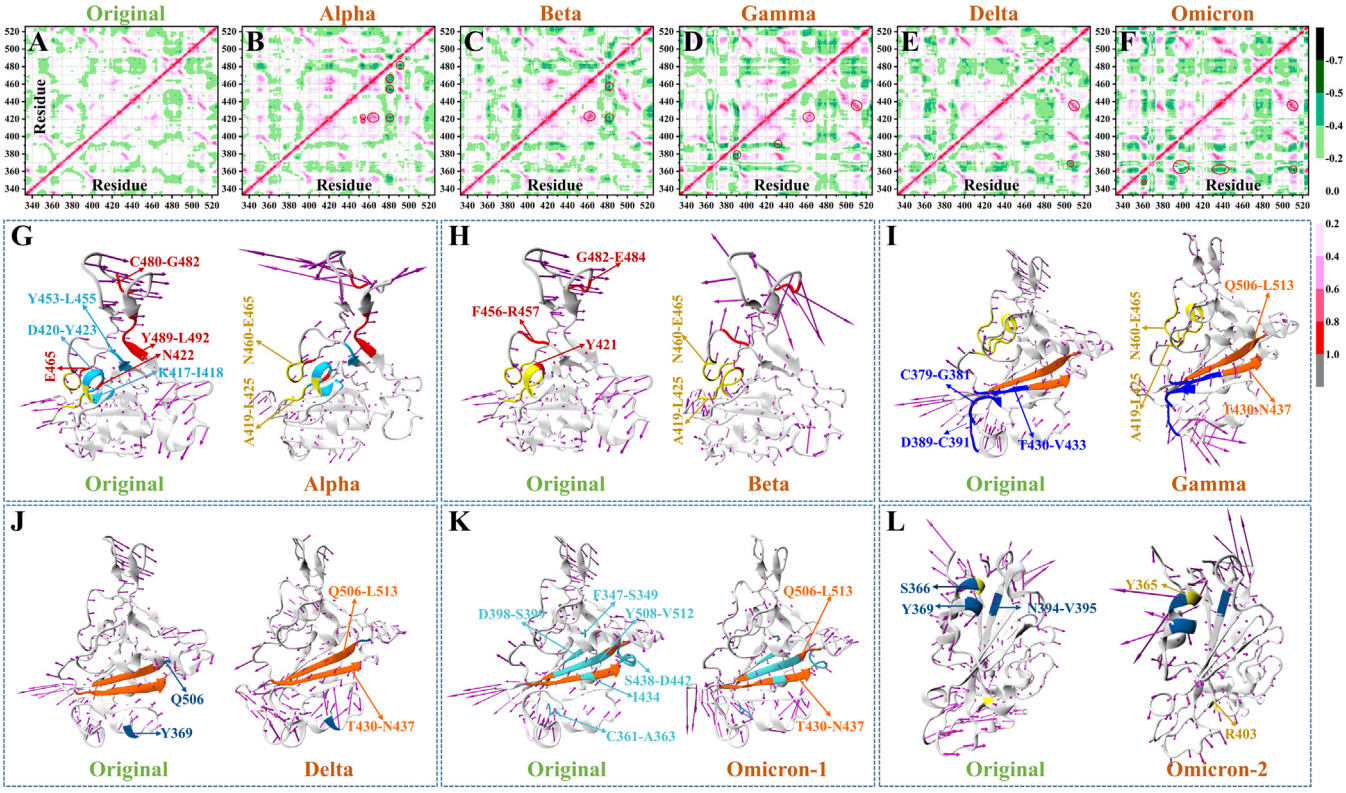


**Fig. 1.** Dynamic cross-correlation matrices and porcupine plots of RBDs. Correlation of residues in RBDs of: (A) original SARS-CoV-2, (B) alpha, (C) beta, (D) gamma, (E) delta and (F) omicron variants. Correlated and anti-correlated movements between residues are shown in red and green, respectively. Comparison of movement strength and direction of residues between the original SARS-CoV-2 and (G) alpha, (H) beta, (I) gamma, (J) delta and (K-L) omicron variants. All plots are constructed based on the first eigenvector and eigenvalues obtained from the diagonalization of the covariance matrix, the length and direction of the purple arrows indicate the movement strength and direction of residues, respectively.

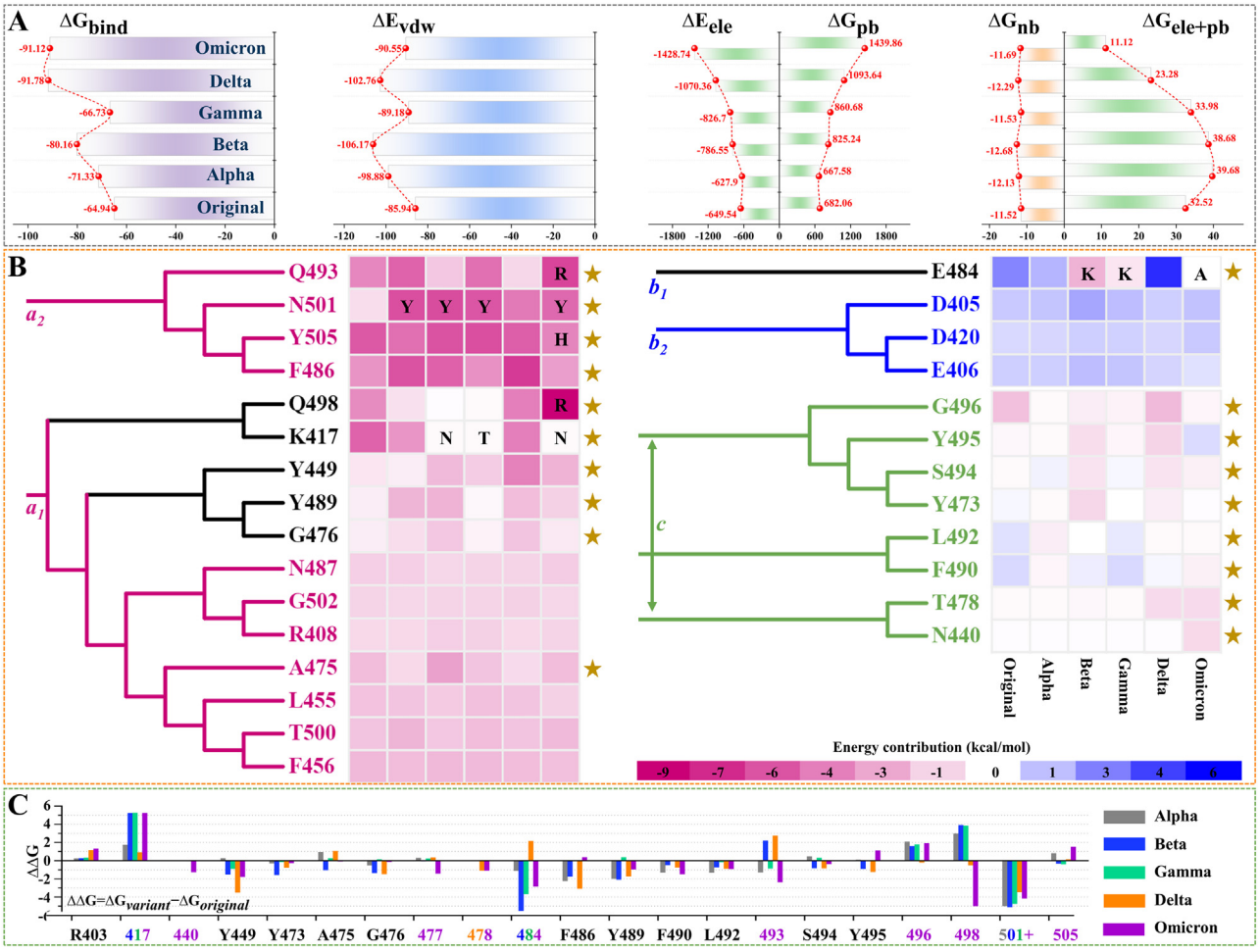


**Fig. 2.** Evaluation of the binding affinity of the original, alpha, beta, gamma, delta and omicron RBDs to ACE2 by MM-PBSA, and residues on RBDs that have important influence on the binding of different SARS-CoV-2 strains to ACE2. (A) Each term of the binding free energy, including total binding free energy ($\Delta G_{bind}$), van der Waals interaction ($\Delta E_{vdw}$), electrostatic interaction ($\Delta E_{ele}$), polar solvation free energy ($\Delta G_{pb}$), non-polar solvation free energy ($\Delta G_{np}$) and the superposition ($\Delta G_{ele+pb}$) of $\Delta E_{ele}$ and $\Delta G_{pb}$. (B) Residues with significant energy contribution to RBD-ACE2 binding, and the residues that are favorable and unfavorable for RBD-ACE2 binding are shown in pink and blue, respectively. Residues that are more affected by mutation are marked with a yellow "⋆". (C) Detailed energy changes of residues that are key contributors to the differences in receptor-binding ability between the mutant and original SARS-CoV-2 strains. All values are in kcal/mol.

$Y501^N$ in omicron RBD, and S19, D30, H34, E35, E37, D38 and D355 in ACE2) key differential residues, respectively (Fig. 2B and Supplementary Figs. 5–7).

Based on the above studies, we aimed to design a short peptide to perturb the binding of different SARS-CoV-2 strains to ACE2, thereby achieving the purpose of blocking or weakening viral infection. The corresponding flowchart and description are shown in Supplementary Fig. 8. After stability assessment, residue mutation[7,8] and MD simulations, the pan-coronavirus short peptide (QWKTFLEKFNH) containing a double mutation (D30E+A25W) was found to be the optimal one among all the designed peptides. We suggest that the peptide inhibitor can directly enter sites that are highly susceptible to virus invasion and infection by intranasal delivery or inhalation, which can not only improve the effect of the peptide, but also reduce the possibility of harmful side effects.

## Declaration of Competing Interest

All authors claim no conflict of interest.

## Acknowledgments

This work was supported by the National Key Research and Development Program of China [Grant No. 2018YFA0903700]; and the National Natural Science Foundation of China [Grant No. 21621004 and 31571358]. The authors would like to thank Prof. Chun-Ting Zhang for the invaluable assistance and inspiring discussions.

## Supplementary materials

Supplementary material associated with this article can be found, in the online version, at doi:10.1016/j.jinf.2022.09.011.

## References

1. Fantini J, Yahi N, Azzaz F, Chahinian H. Structural dynamics of SARS-CoV-2 variants: a health monitoring strategy for anticipating Covid-19 outbreaks. *J Infect* 2021;**83**:197–206.
2. World Health Organization. COVID-19 weekly epidemiological update, 25 February 2021. https://www.who.int/publications/m/item/covid-19-weekly-epidemiological-update, 2021.
3. Chen JZ, Wang XY, Pang LX, Zhang JZH, Zhu T. Effect of mutations on binding of ligands to guanine riboswitch probed by free energy perturbation and molecular dynamics simulations. *Nucleic Acids Res* 2019;**47**:6618–31.
4. Wang Q, Zhang Y, Wu L, Niu S, Song C, Zhang Z, et al. Structural and functional basis of SARS-CoV-2 entry by using human ACE2. *Cell* 2020;**181**:894–904 e899.
5. Yan FF, Gao F. Comparison of the binding characteristics of SARS-CoV and SARS–CoV-2 RBDs to ACE2 at different temperatures by MD simulations. *Brief Bioinform* 2021;**22**:1122–36.
6. Mannar D, Saville James W, Zhu X, Srivastava Shanti S, Berezuk Alison M, Tuttle Katharine S, et al. SARS-CoV-2 omicron variant: antibody evasion and cryo-EM structure of spike protein–ACE2 complex. *Science* 2022;**375**:760–4.

7. Marqusee S, Baldwin RL. Helix stabilization by Glu-...Lys+ salt bridges in short peptides of de novo design. *Proc Natl Acad Sci* 1987;**84**:8898–902.
8. Rodrigues CHM, Myung Y, Pires DEV, Ascher DB. mCSM-PPI2: predicting the effects of mutations on protein–protein interactions. *Nucleic Acids Res* 2019;**47**:W338–44.

Fangfang Yan
*Department of Physics, School of Science, Tianjin University, Tianjin 300072, China*

Feng Gao*
*Department of Physics, School of Science, Tianjin University, Tianjin 300072, China*
*Frontiers Science Center for Synthetic Biology and Key Laboratory of Systems Bioengineering (Ministry of Education), Tianjin University, Tianjin 300072, China*
*SynBio Research Platform, Collaborative Innovation Center of Chemical Science and Engineering (Tianjin), Tianjin 300072, China*

*Corresponding author at: Department of Physics, School of Science, Tianjin University, Tianjin, China.
*E-mail address:* fgao@tju.edu.cn (F. Gao)